SIAM J. APPL. MATH.
Vol. 73, No. 5, pp. 1941–1957

HYPERBOLIC THEORY FOR FLOW IN PERMEABLE MEDIA WITH PH-DEPENDENT ADSORPTION*

VALENTINA PRIGIOBBE†, MARC A. HESSE‡, AND STEVEN L. BRYANT§

Abstract. A theory for the solution of the Riemann problem for a one-dimensional, quasi-linear, 2×2 system of conservation laws describing reactive transport in a permeable medium with pH-dependent adsorption is developed. The system is strictly hyperbolic and nongenuinely nonlinear because the adsorption isotherms are not convex functions. The solution comprises nine fundamental structures, which are a concatenation of elementary and composed waves. In the limit of low pH, the isotherms reduce to convex two-component Langmuir isotherms considered in chromatography, and the solution comprises only four fundamental structures, as in classical theory. Semianalytical solutions and highly resolved numerical simulations show good agreement in all cases.

Key words. chromatography, conservation laws, hyperbolic partial differential equations, non-genuinely nonlinear, pH-dependent adsorption, porous media, reactive transport

AMS subject classifications. 35L02, 35L40, 35L60, 35L65, 35L67, 35Q99

DOI. 10.1137/130907185

1. Introduction.

In this paper, a theory for the solution of the Riemann problem of a 2×2 system of conservation laws describing reactive transport in a permeable medium with pH-dependent adsorption is discussed. The suitably nondimensionalized conservation laws for the total concentration of protons, c_{ht}, and the concentration of a charged solute, c_s, in an incompressible and isothermal fluid in local chemical equilibrium are given by

$$\mathbf{a}(\mathbf{c})_t + \mathbf{c}_x = 0 \quad \text{on} \quad -\infty < x < \infty,\ t > 0, \tag{1.1}$$

where $\mathbf{c} = (c_{ht}, c_s)$, and the piecewise constant initial data

$$\mathbf{c}(x,0) = \begin{cases} \mathbf{c}^l & \text{for } x < 0, \\ \mathbf{c}^r & \text{for } x > 0 \end{cases} \tag{1.2}$$

are defined by the left and right states. The nonlinear coupling between the equations arises in the accumulation term,

$$\mathbf{a}(\mathbf{c}) = \mathbf{c} + \mathbf{z}(\mathbf{c}), \tag{1.3}$$

*Received by the editors January 24, 2013; accepted for publication (in revised form) July 15, 2013; published electronically October 24, 2013. This material is based upon work supported as part of the Center for Frontiers of Subsurface Energy Security (CFSES), an Energy Frontier Research Center funded by the U.S. Department of Energy, Office of Science, Office of Basic Energy Sciences under Award DE-SC0001114. Acknowledgment is made to the Donors of the American Chemical Society Petroleum Research Fund, for partial support of this research.
http://www.siam.org/journals/siap/73-5/90718.html

†Department of Petroleum and Geosystems Engineering, University of Texas at Austin, Austin, TX 78712 (valentina.prigiobbe@austin.utexas.edu).

‡Department of Geosciences and Institute for Computational Engineering and Sciences, University of Texas at Austin, Austin, TX 78712 (mhesse@jsg.utexas.edu).

§Department of Petroleum and Geosystems Engineering and Institute for Computational Engineering and Sciences, University of Texas at Austin, Austin, TX 78712 (steven_bryant@mail.utexas.edu).

which contains the absorbed concentrations, $\mathbf{z}(\mathbf{c}) = (z_h(\mathbf{c}), z_s(\mathbf{c}))$, also referred to as adsorption isotherms, given by

$$z_h = \frac{\phi z_t k_h \frac{1}{2}\left(c_{ht} + \sqrt{c_{ht}^2 + 4k_w}\right)}{1 + k_h \frac{1}{2}\left(c_{ht} + \sqrt{c_{ht}^2 + 4k_w}\right) + k_s c_s}, \tag{1.4}$$

$$z_s = \frac{\phi z_t k_s c_s}{1 + k_h \frac{1}{2}\left(c_{ht} + \sqrt{c_{ht}^2 + 4k_w}\right) + k_s c_s}, \tag{1.5}$$

where k_h and k_s are the equilibrium constants for the adsorption of protons and the solute, k_w is the dissociation constant of water, z_t is the total concentration of adsorption sites, and ϕ is the dimensionless ratio of solid to fluid volume. Without loss of generality, throughout the paper we assume the following values: $k_h = 10^8$, $k_s = 10^5$, $k_w = 10^{-14}$, $z_t = 10^{-2}$, and $\phi = 0.4$. The derivation of the governing equations and isotherms is outlined in Appendix B. Figure 1 shows the adsorption isotherms in composition space, also called the hodograph plane, which is spanned by c_{ht}/k and c_s/k, where $k = (k_h - k_s)/(k_h k_s)$ [29]. The isotherms show the rapid changes in the absorbed concentrations near the c_s-axis, the so-called sorption-edges. Note that c_{ht} can attain both positive and negative values while c_s is nonnegative (Appendix A).

The analysis presented here builds on the analytic solutions for competitive adsorption and ion-exchange in chemical engineering processes [11, 32, 13, 29, 23] and its applications to fluid flow in the subsurface [26, 33, 7, 2, 3, 8, 18]. The pH of the solution has a strong effect on the adsorption of solutes and, therefore, on solute transport in reactive permeable media. Previous work on analytical solutions for solute transport with pH-dependent adsorption has used charge balance to eliminate the proton concentration [10, 27]. During adsorption, charges can build up at the solid-liquid interface and strict charge balance cannot be assumed so that the conservation of protons has to be modeled explicitly [12, 22]. The conservation equation for protons contains a term accounting for the dissociation of water, which introduces additional nonlinearity in the accumulation term and renders the hyperbolic system nongenuinely nonlinear. This additional nonlinearity fundamentally changes the structure of the theoretical development and gives rise to new types of solutions that are not present in previous work on adsorption. Here, semianalytical solutions to the Riemann problem are developed and compared with highly resolved numerical simulations.

2. Self-similar solution. The weak solution of the Riemann problem for hyperbolic systems is invariant under a uniform stretching transformation of the independent variables ($\bar{x} = e^{\alpha}x$, $\bar{t} = e^{\alpha}t$) [6], so a self-similar solution in the similarity variable $\eta := x/t$ is sought. The similarity transformation reduces the system of partial differential equations (1.1) to the following system of ordinary differential equations:

$$\left(\nabla_c \mathbf{a}(\mathbf{c}) - \frac{1}{\eta}\mathbf{I}\right)\frac{\mathrm{d}\mathbf{c}}{\mathrm{d}\eta} = 0, \tag{2.1}$$

which is in the form of a nonlinear eigenvalue problem, with eigenvalue $\sigma_p(\mathbf{c}) = 1/\eta = t/x$ and the eigenvectors $\mathbf{r}_p(\mathbf{c}) = \mathrm{d}\mathbf{c}/\mathrm{d}\eta$. The similarity transformation asserts that $\mathbf{c}$ is constant along trajectories which propagate at the constant velocity, $v_p = 1/\sigma_p = \eta$. The interpretation of the eigenvalue, $\sigma_p(\mathbf{c})$, is therefore the retardation of $\mathbf{c}$. The

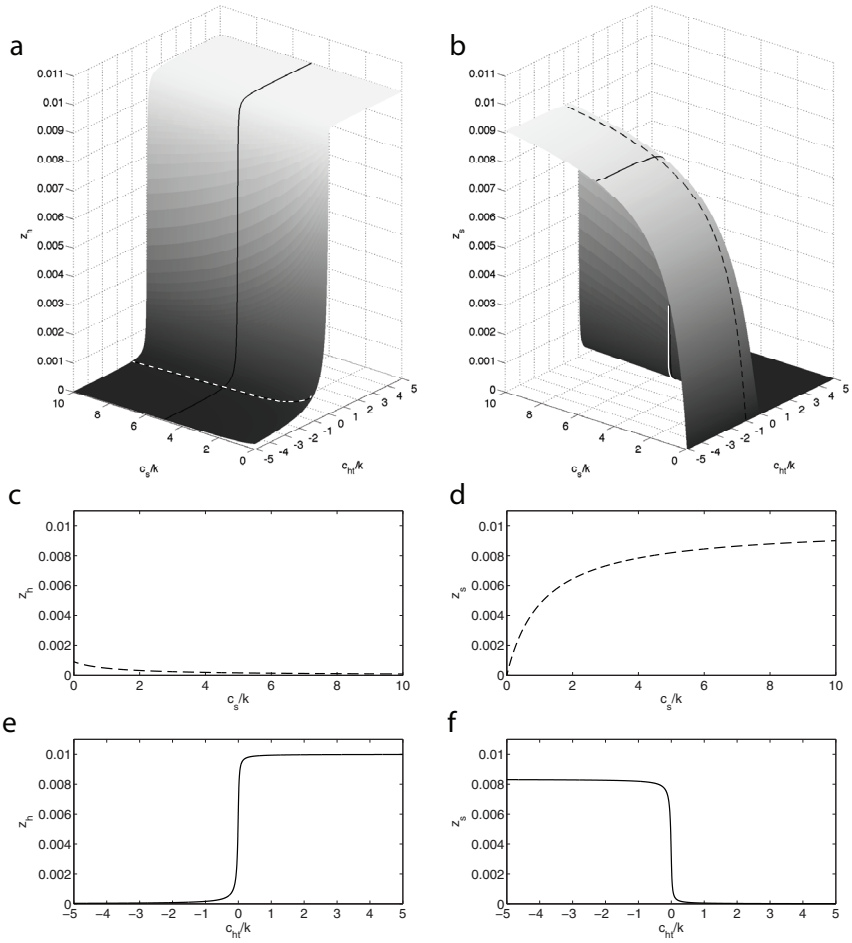

FIG. 1. *Variation of the adsorption isotherms in composition space and two-dimensional sections along $c_s/k = 5$ and $c_{ht}/k = -1$ in solid and dashed lines, respectively.*

retardation arises instead of the velocity, because the nonlinearity in (1.1) is in the accumulation term instead of in the flux term [29, 20]. In chromatography [23], it is common to express (2.1) in terms of the gradient of the absorbed concentrations, $\nabla_c \mathbf{z}$, and its eigenvalues, $\theta_p = \sigma_p - 1$, so that

$$(\nabla_c \mathbf{z} - \theta_p \mathbf{I})\, \mathbf{r}_p = 0. \tag{2.2}$$

The eigenvalues of (2.1) are given by

$$\theta_p = \frac{1}{2}\left(z_{s,s} + z_{h,ht} \pm \sqrt{\Delta}\right) \quad \text{and} \quad \sigma_p = 1 + \theta_p, \tag{2.3}$$

where $\Delta = (z_{s,s} - z_{h,ht})^2 + 4 z_{h,s} z_{s,ht}$ is the discriminant and $z_{i,j}$ is the partial derivative of the isotherm z_i with respect to c_j. The eigenvalues as a function of the normalized compositions c_{ht} and c_s are shown in Figure 2.

For competitive adsorption, the cross-derivatives of the isotherms, $z_{h,s}$ and $z_{s,ht}$, are generally negative [29, 23]. The sign of the cross-derivatives is clear when the concentration of protons,

$$c_h = \frac{1}{2}\left(c_{ht} + \sqrt{c_{ht}^2 + 4k_w}\right) > 0, \tag{2.4}$$

is identified in the isotherms (1.4) and (1.5), and $z_h(c_h, c_s)$ and $z_s(c_h, c_s)$ are recognized as standard Langmuir isotherms, with negative cross-derivatives, $z_{h,s}$ and $z_{s,h}$ [29]. For the pH-dependent case considered here, $z_{s,ht} = z_{s,h}c_{h,ht} < 0$, because

$$c_{h,ht} = \frac{1}{2} + \frac{c_h}{\sqrt{c_{ht}^2 + 4k_w}} > 0. \tag{2.5}$$

Therefore, the discriminant, Δ, is positive, and the two eigenvalues θ_p are real, distinct, and positive. Because the eigenvalues represent retardations, they are sorted in decreasing order, $\theta_1 > \theta_2$, to maintain standard ordering of the waves from the slowest to the fastest [20]. This implies that the 2×2 quasi-linear system (2.1) is strictly hyperbolic [19] and the isotherms are physically admissible [23]. The theory of hyperbolic systems with genuinely nonlinear fields was developed by Lax [19] and then extended by Liu [21] to systems with nongenuinely nonlinear fields. This extended theory will be used here to describe the admissible wave structure and the complete set of analytical solutions of the Riemann problem. To define the physically correct, unique, weak solution of the hyperbolic problem given by (1.1), an appropriate entropy condition must be satisfied [20].

3. Wave structure and hodograph plane. The weak solution of the Riemann problem for a strictly hyperbolic 2×2 system consists of a concatenation of two waves, $\mathcal{W}_1$ (slow wave) and $\mathcal{W}_2$ (fast wave), connecting three constant states, $\mathbf{c}^l$ (left state), $\mathbf{c}^m$ (middle state), and $\mathbf{c}^r$ (right state)

$$\mathbf{c}^l \xrightarrow{\mathcal{W}_1} \mathbf{c}^m \xrightarrow{\mathcal{W}_2} \mathbf{c}^r. \tag{3.1}$$

The construction of the solution requires the determination of two waves and the location of the middle state in the hodograph plane, the space of dependent variables. In reactive transport problems, the dependent variables are the compositions and, therefore, the hodograph plane is referred to as composition space and the waves are said to follow composition paths [13, 26, 18, 25].

3.1. Integral curves and rarefaction waves. Rarefactions are elementary waves connecting two constant states with a smooth variation in concentration. The composition paths of p-rarefactions, $\mathcal{R}_p$, are the integral curves of the pth eigenvector of (2.1), given by

$$\mathbf{c}_p(\mathbf{c}^0, \eta) = \mathbf{c}^0 + \int_0^\eta \mathbf{r}_p(\mathbf{c})\, \mathrm{d}\eta', \tag{3.2}$$

where the eigenvectors are

$$\mathbf{r}_p = \left(\frac{\mathrm{d}\mathbf{c}}{\mathrm{d}\eta}\right)_p = \begin{pmatrix} z_{s,ht} \\ \sigma_p - 1 - z_{s,s} \end{pmatrix}. \tag{3.3}$$

The two families of integral curves of (2.1) depicted in Figure 2 show two distinct patterns for negative and positive values of c_{ht}, which are separated by a transition

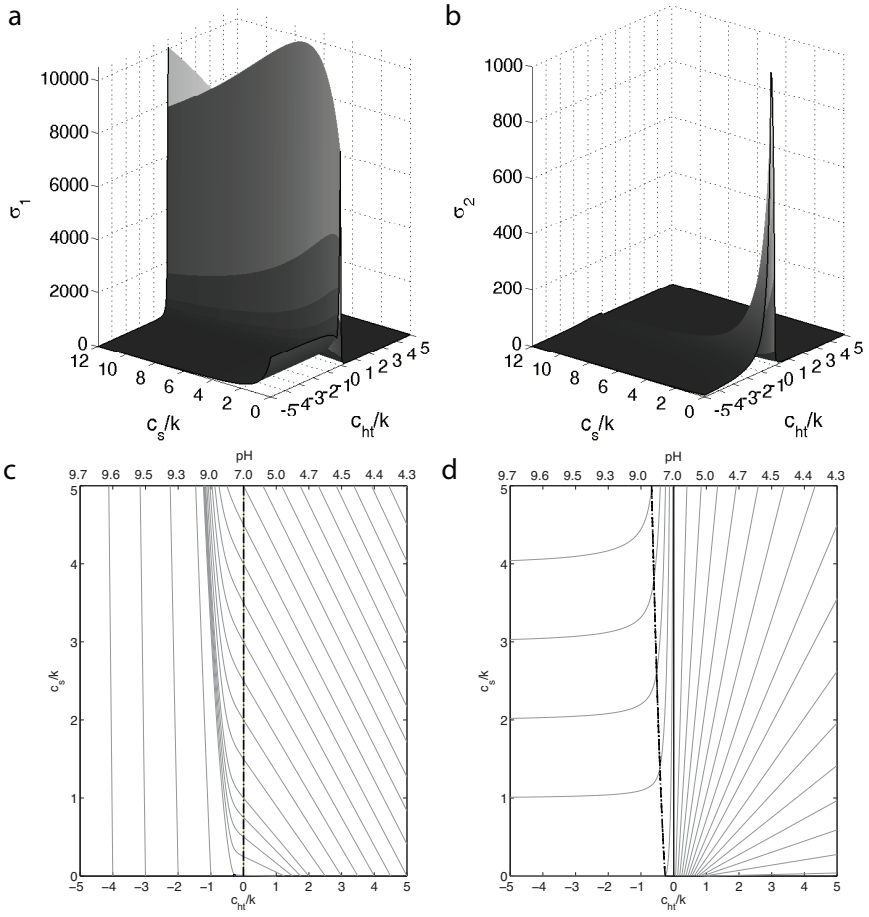

FIG. 2. *The eigenvalues, the integral curves, and the inflection loci in the hodograph plane.* (a) *Eigenvalue* σ_1*;* (b) *eigenvalue* σ_2*;* (c) *slow paths (gray) and inflection locus* I_1 *(black dashed line);* (d) *fast paths (gray) and inflection locus* I_2 *(black dash-and-dot line).*

region centered near $c_{ht} = 0$. Far from the c_s-axis the integral curves form nets of intersecting straight lines, but in the transition region they become strongly curved and approach vertical asymptotes. The complexity of the integral curves in the transition region is a reflection of the rapid changes in the sorbed concentrations that is a characteristic of pH-dependent adsorption.

The rarefaction waves are physically admissible if the retardation, σ_p, decreases monotonically along the composition path from the left to the right. Figure 2 shows that the σ_p's are not monotonic functions near the c_s-axis, which leads to the occurrence of composite waves discussed in section 3.3.

3.2. Hugoniot locus and shock waves. Shocks are elementary waves connecting two constant states, $\mathbf{c}^-$ and $\mathbf{c}^+$, with a discontinuous variation in composition. Mass conservation requires that the retardation of a shock, $\tilde{\sigma}_p$, must satisfy the

Rankine–Hugoniot jump condition

$$\tilde{\sigma}_p(\mathbf{c}^-, \mathbf{c}^+) = \frac{[\mathbf{a}(\mathbf{c})]}{[\mathbf{c}]} = 1 + \frac{[\mathbf{z}(\mathbf{c})]}{[\mathbf{c}]}, \tag{3.4}$$

where the brackets indicate the difference between the two states across the discontinuity [29, 20]. Again, the retardation arises naturally, instead of the velocity, because the nonlinearity is in the accumulation term instead of in the flux term.

For a given state $\mathbf{c}^-$, the jump condition defines two lines in composition space, the Hugoniot locus $\mathcal{H}(\mathbf{c}^-)$, that give the set of all $\mathbf{c}^+$ that can be connected to $\mathbf{c}^-$ through a mass-conserving shock, $\mathcal{S}_p$. The two lines comprising $\mathcal{H}(\mathbf{c}^-)$ are tangent to the integral curves at $\mathbf{c}^-$, but they deviate significantly from the integral curves in the transition region near the c_s-axis, as shown in Figures 3a and 3b. This is important for the construction of the solution, if $\mathbf{c}^l$ and $\mathbf{c}^r$ lie on opposite sides of the c_s-axis and their integral curves do not intersect.

A p-shock is physically admissible if it satisfies the Lax entropy condition [19]

$$\sigma_p(\mathbf{c}^-) > \tilde{\sigma}_p(\mathbf{c}^-, \mathbf{c}^+) > \sigma_p(\mathbf{c}^+), \tag{3.5}$$

which ensures that the shock is self-sharpening and therefore stable. Figure 3 shows the portions of the $\mathcal{H}(\mathbf{c}^-)$ that satisfies (3.5) as solid lines. Due to the nonmonotonic variation of σ_p, a single branch of $\mathcal{H}(\mathbf{c}^-)$ can satisfy (3.5) only along segments, which leads to the occurrence of composite waves discussed in section 3.3.

Figure 3c shows that $\mathcal{H}(\mathbf{c}^-)$ can have three branches, two attached to $\mathbf{c}^-$ and a detached branch. The presence of the detached branch is an interesting feature of systems with pH-dependent adsorption, which is essential for the construction of the solution in some cases where $\mathbf{c}^-$ and $\mathbf{c}^+$ lie on opposite sides of the transition region near the c_s-axis. Detached branches have only been reported for relatively few physical systems modeled by hyperbolic conservation laws [17, 4, 9, 15], and have not been previously reported for reactive transport. Figure 3d shows the area on the hodograph plane, where detached branches of $\mathcal{H}(\mathbf{c}^-)$ that satisfy the entropy condition exist. The extent of this area will vary with k_s and k_h, but its existence for negative values of c_{ht} is a general feature of reactive transport with pH-dependent adsorption. Thus, this type of behavior constitutes a nontrivial generalization of classical theories of transport with competitive adsorption.

3.3. Inflection locus and shock-rarefaction waves. In systems with pH-dependent adsorption both characteristic fields are nongenuinely nonlinear, because the σ_p's are not monotonic functions of composition, as shown in Figure 2. Therefore, each p-wave may consist of a combination of rarefactions and shocks [21].

The inflection locus I_p for the pth characteristic field gives the locations where σ_p attains a maximum value when moving along integral curves of the p-family and it is defined as

$$\nabla \sigma_p \cdot \mathbf{r}_p = 0. \tag{3.6}$$

The inflection loci for both characteristic fields are single connected curves indicated with black dash-and-dot lines on the hodograph plane shown in parts (c) and (d) of Figure 2.

A composed p-wave arises when it joins two states on opposite sides of the corresponding inflection locus, I_p. The order of the shock and the rarefaction in the composed wave is determined by the nature of the local extremum of σ_p [1]. The

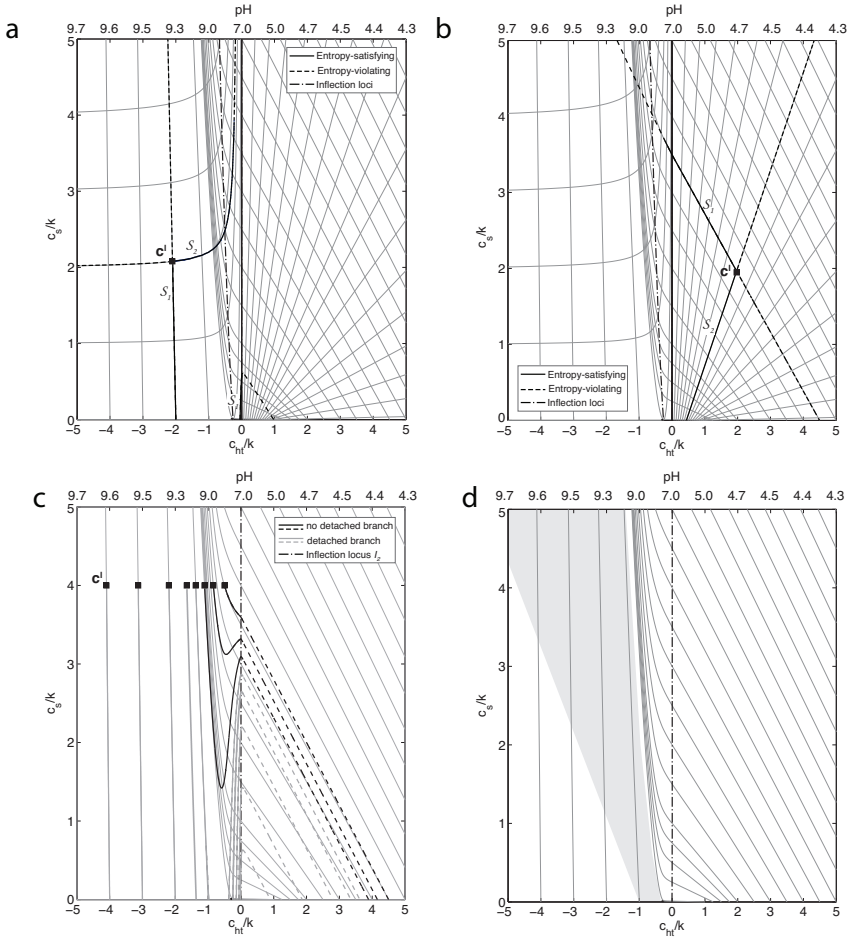

FIG. 3. *Hugoniot loci.* (a) *and* (b) *Hugoniot loci emanating from a left state,* $\mathbf{c}_l$*, in the left and right halves of the hodograph plane, respectively.* (c) *The attached and detached branches of the hugoniot locus* $\mathcal{H}_1$ *for left states with increasing pH.* (d) *The region in the hodograph plane where the* $\mathcal{H}_1$ *of a left state has a detached branch.*

inflection loci shown in Figure 2 correspond to local maxima of σ_p, which correspond to minima in the velocity, so that with the rarefaction the inflection loci is always slower than the shock. The shock-rarefaction of the pth family connecting two constant states, $\mathcal{SR}_p$, is a curve consisting of a p-shock emanating from $\mathbf{c}^-$, connected at an intermediate point $\mathbf{c}^*$ to a p-rarefaction, which ends at $\mathbf{c}^+$. Any discontinuity $\mathcal{S}_p$ connecting the states $\mathbf{c}^-$ and $\mathbf{c}^*$ must satisfy the Liu entropy condition [21] given by

$$\sigma_p(\mathbf{c}^-) \geq \sigma_p(\mathbf{c}^-, \mathbf{c}^*) > \sigma_p(\mathbf{c}^+). \tag{3.7}$$

4. Fundamental structure of the solutions of the Riemann problem. The nine fundamental structures of the solutions of the Riemann problem are illustrated in this section in the same fashion as in [16]. The solutions are a concatenation of the entropy-satisfying waves of rarefaction, shock, and shock-rarefaction as listed in Table 1. The nine fundamental entropy-satisfying weak solutions of the Riemann problem are shown together with the numerical simulations for a representative set of

TABLE 1

Complete set of the fundamental structures of the solutions of the Riemann problem comprising four concatenations of elementary waves, four concatenations of composed waves and elementary waves, and one concatenation of two composed waves.

Solution	$\mathcal{W}_1$	$\mathcal{W}_2$	Illustration
1	$\mathcal{S}_1$	$\mathcal{S}_2$	Figure 4(a–c)
2	$\mathcal{R}_1$	$\mathcal{R}_2$	Figure 4(d–f)
3	$\mathcal{R}_1$	$\mathcal{S}_2$	Figure 4(g–i)
4	$\mathcal{S}_1$	$\mathcal{R}_2$	Figure 5(a–c)
5	$\mathcal{SR}_1$	$\mathcal{R}_2$	Figure 5(d–f)
6	$\mathcal{SR}_1$	$\mathcal{S}_2$	Figure 5(g–i)
7	$\mathcal{S}_1$	$\mathcal{SR}_2$	Figure 6(a–c)
8	$\mathcal{R}_1$	$\mathcal{SR}_2$	Figure 6(d–f)
9	$\mathcal{SR}_1$	$\mathcal{SR}_2$	Figure 6(g–h)

left and right states in Figures 4 through 6. They are illustrated as composition paths on the hodograph plane and as concentration profiles as a function of the similarity variable η.

The numerical solutions were calculated using a finite volume scheme for the discretization of the nonlinear system given in (1.1). The accumulation term was not expanded, but differentiated directly to treat the nonlinearity implicitly, and the advection term was integrated explicitly and approximated with an upwind flux [27]. All numerical solutions presented in this paper use a dimensionless domain of length 0.2 divided into 3000 uniform grid cells. The Courant number for the initial time step was unity. To ensure convergence of the Newton iteration, the time step was reduced adaptively.

5. Discussion.

5.1. Comparison with the theory of chromatography. For positive values of c_{ht}, i.e., pH lower than 7, the difference between c_{ht} and c_h is negligible and the conservation laws given in (1.1) simplify to

$$\frac{\partial}{\partial t}\left(c_h + z_h\right) + \frac{\partial c_h}{\partial x} = 0, \tag{5.1}$$

$$\frac{\partial}{\partial t}(c_s + z_s) + \frac{\partial c_s}{\partial x} = 0, \tag{5.2}$$

and the adsorption isotherms reduce to two-component Langmuir adsorption isotherms,

$$z_h = \frac{\phi c_h k_h z_t}{1 + c_h k_h + c_s k_s}, \tag{5.3}$$

$$z_s = \frac{\phi c_s k_s z_t}{1 + c_h k_h + c_s k_s}, \tag{5.4}$$

used in the theory of chromatography [11, 32, 13, 29, 18, 23]. The two-component Langmuir isotherms are concave functions and systems (5.1)–(5.4) are genuinely nonlinear, so that the fundamental structures of the analytical solutions of the Riemann problem are four concatenations of elementary waves corresponding to the first four types given in Table 1. The nongenuine nonlinearity of pH-dependent adsorption, therefore, introduces two inflection loci and adds five additional solution structures involving composed waves.

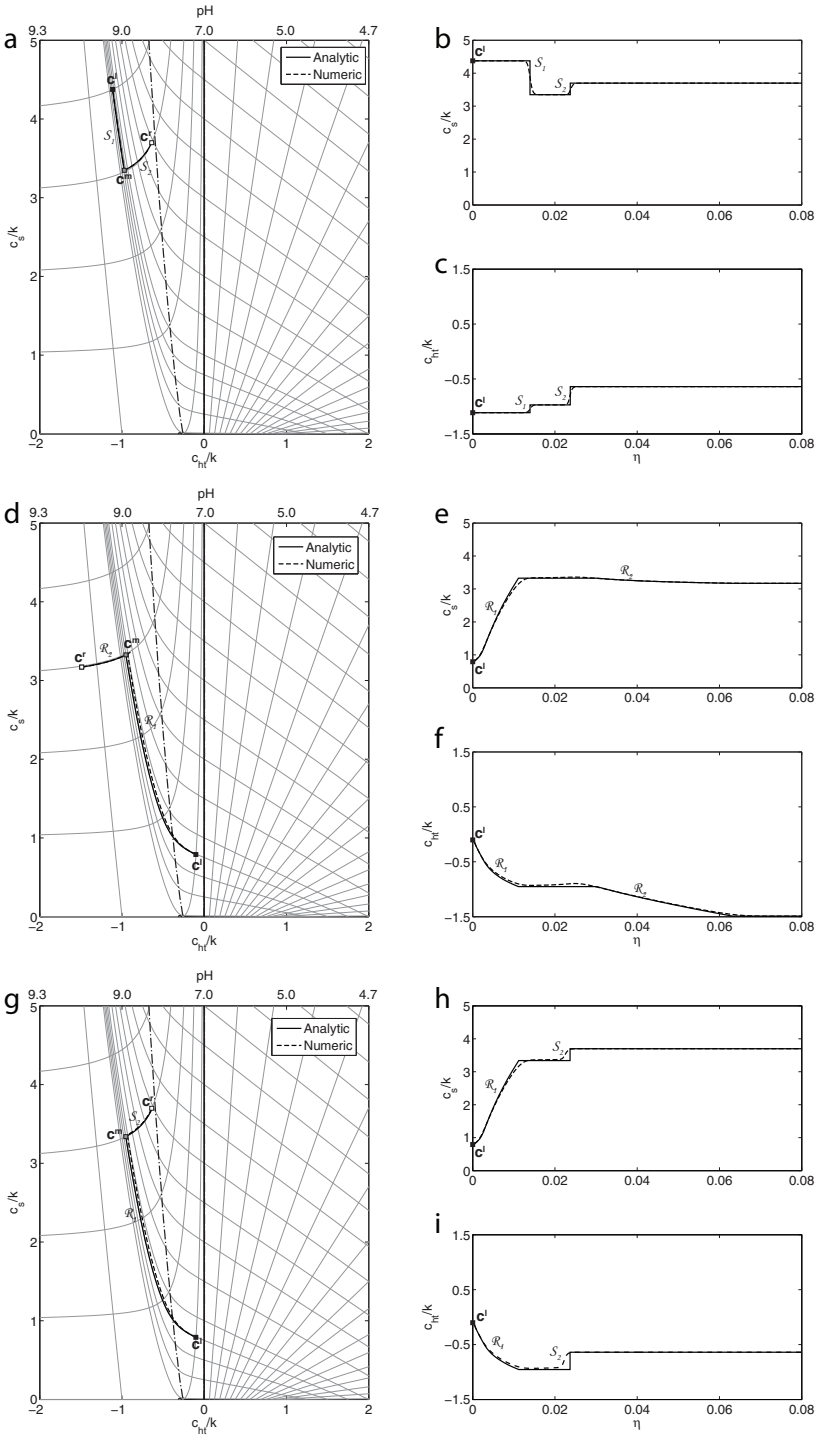

FIG. 4. *Fundamental structures of the solutions* 1–3 *as in Table* 1.

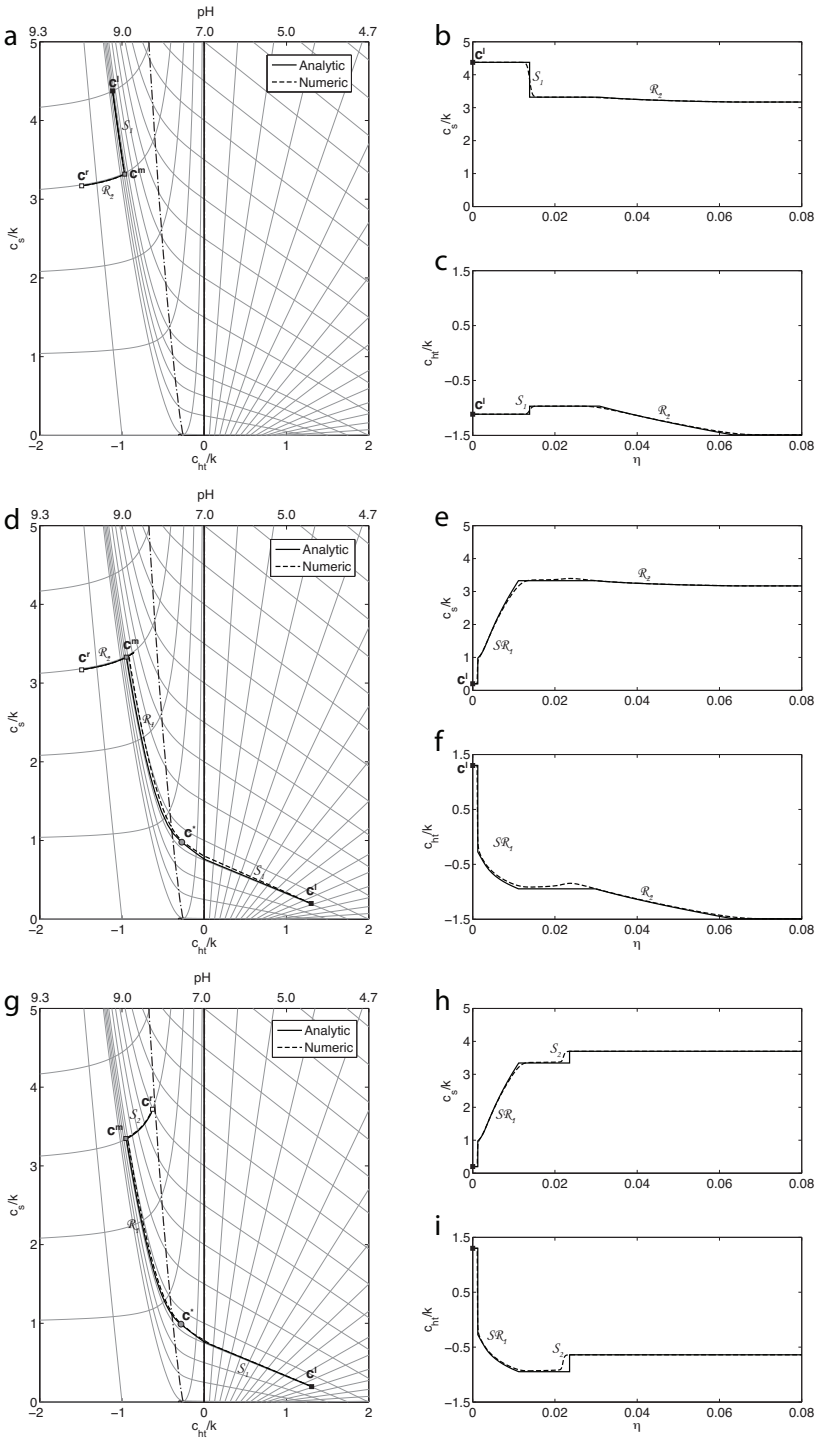

FIG. 5. *Fundamental structures of the solutions* 4–6 *as in Table* 1.

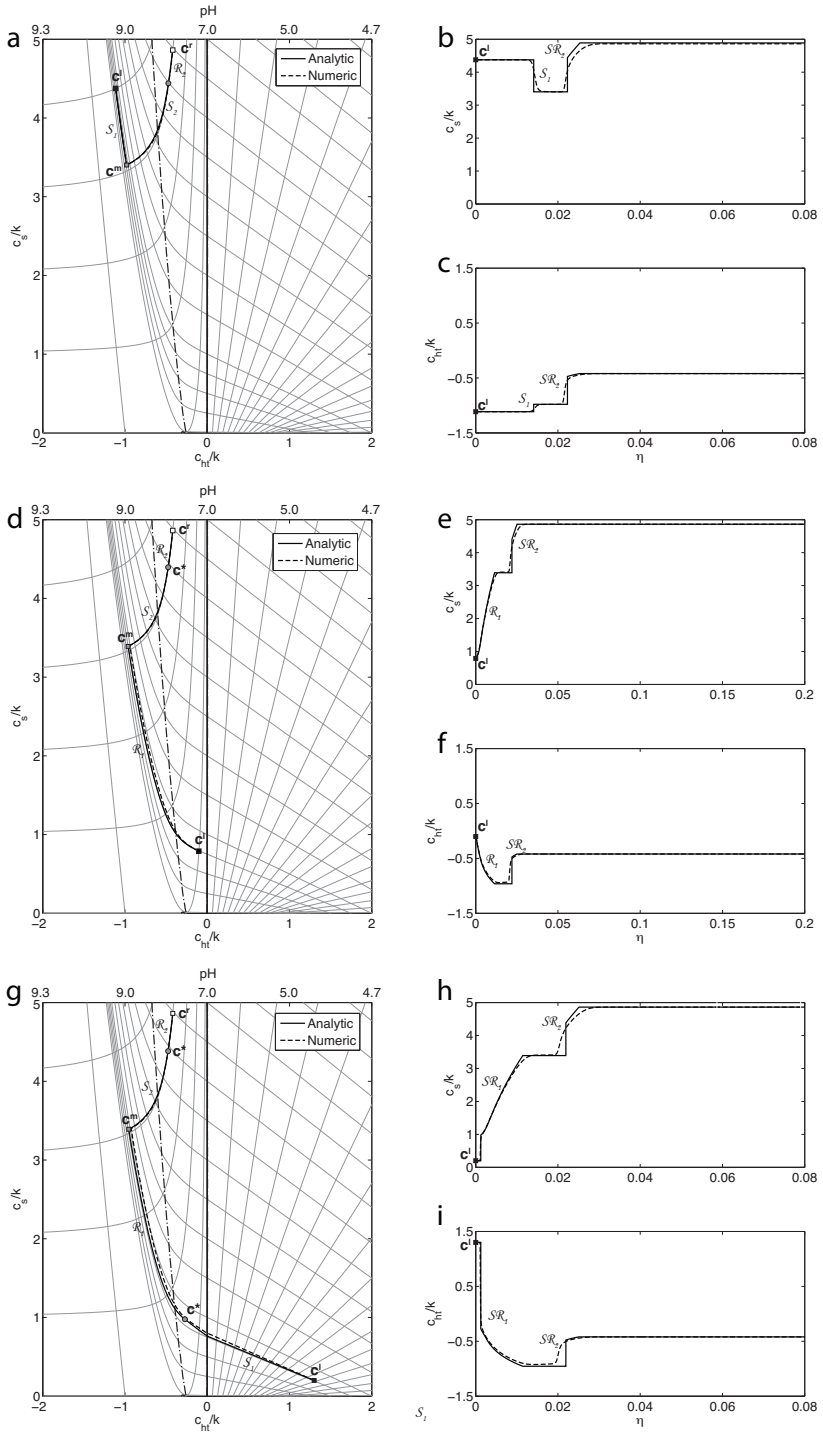

FIG. 6. *Fundamental structures of the solutions* 7–9 *as in Table* 1.

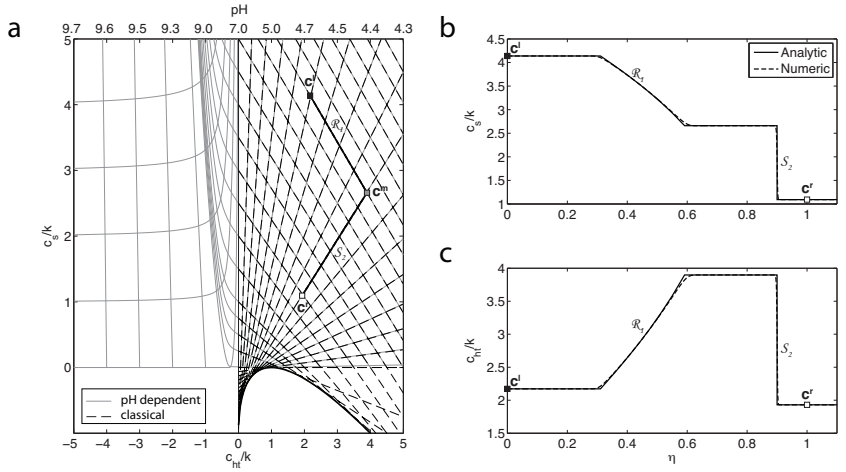

FIG. 7. (a) *Comparison of the integral curves for pH-dependent adsorption shown in solid gray lines and for classical chromatography shown as dashed black lines* [29]. *The analytical and numerical solutions, for a particular set of* $\mathbf{c}^l$ *and* $\mathbf{c}^r$, *are shown as a composition path in the hodograph plane,* (a)*, and as concentration profiles,* (b) *and* (c).

Figure 7 shows that the integral curves for pH-dependent adsorption coincide with the integral curves from the theory of chromatography for $c_{ht} > 0$ [29]. Here, the integral curves have been shown to be straight lines that are tangent to a parabolic envelope curve in the fourth quadrant of the hodograph plane. Therefore, system (5.1)–(5.4) are of Temple-class [30] and the Hugoniot loci are identical to the corresponding integral curves. In pH-dependent adsorption, this simplification is not generally valid, and the Hugoniot loci can deviate significantly from the integral curves and even have detached branches as illustrated in section 3.2.

5.2. The effect of pH on the solution structure. To illustrate the strong effect of pH variations on the structure of the concentration fronts, we consider a sequence of solutions with a fixed right state, $\mathbf{c}^r$, at pH= 5.0 and a sequence of left states, $\mathbf{c}^l$, with fixed c_s^l but decreasing c_{ht}^l, corresponding to a pH increasing from 4.9 to 9.6. The gradual change of the structure of the analytical solution of the Riemann problem is shown in Figure 8. As the pH of the left state increases, the fundamental structure of the solution changes as follows:

1. $\mathbf{c}^l \xrightarrow{\mathcal{R}_1} \mathbf{c}^m \xrightarrow{\mathcal{S}_2} \mathbf{c}^r$,
2. $\mathbf{c}^l \xrightarrow{\mathcal{SR}_1} \mathbf{c}^m \xrightarrow{\mathcal{S}_2} \mathbf{c}^r$,
3. $\mathbf{c}^l \xrightarrow{\mathcal{SR}_1} \mathbf{c}^m \xrightarrow{\mathcal{R}_2} \mathbf{c}^r$,
4. $\mathbf{c}^l \xrightarrow{\mathcal{S}_1} \mathbf{c}^m \xrightarrow{\mathcal{SR}_2} \mathbf{c}^r$.

Figures 8b and 8c show the smooth variation of the analytical solution with the change in the left state. This illustrates the continuous dependence of the solution on the initial condition (1.2). In particular, it shows that the occurrence of shocks to the detached branch of the Hugoniot locus, in structures 2 and 3, does not cause an abrupt change in the shape of the concentration profiles. This provides evidence for the uniqueness of the solution and indicates the robustness of the mathematical model for pH-dependent adsorption. In practice, this is of importance for applications such as laboratory experiments that aim at reproducing the Riemann problem to test the reactive transport model.

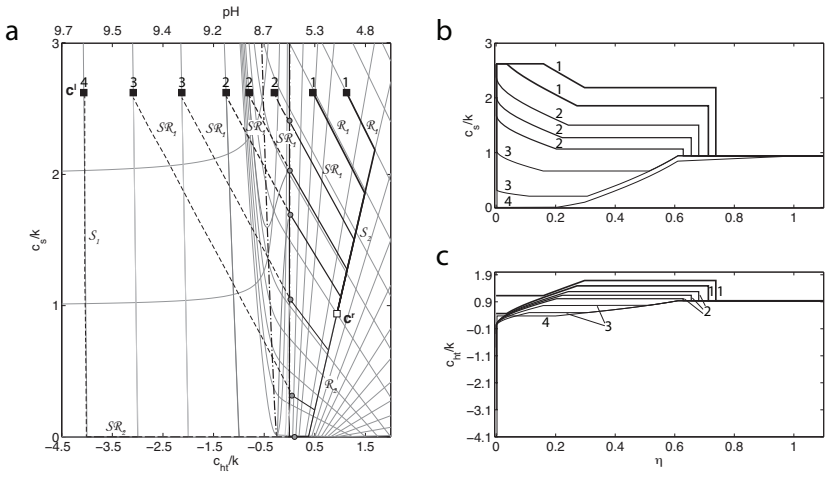

FIG. 8. *Gradual change of the fundamental structure of the analytical solutions of the Riemann problem with the change of the left state. Solutions with the same structure have the same line thickness and the numbers correspond to the four structures discussed in section* 5.2.

5.3. Dispersion-induced waves in pH-dependent reactive transport. For some sets of $\mathbf{c}^l$ and $\mathbf{c}^r$, the combined effect of hydrodynamic dispersion, which adds a diffusive flux, and pH-dependent adsorption leads to the formation of an additional pulse traveling without retardation. This dispersion-induced wave is not present in the analytical solution in the hyperbolic limit [31, 5, 27, 28]. The appearance of this wave in pH-dependent reactive transport is interesting because hydrodynamic dispersion generally only smooths the concentration profiles. This behavior has recently been analyzed under the simplifying assumption of solution charge balance [27] and it is also present in numerical solutions of the more complete model of pH-dependent sorption discussed here.

The dispersion-induced wave arises when $\mathbf{c}^l$ and $\mathbf{c}^r$ are on opposite sides of the transition zone and $c_{ht}^l < c_{ht}^r$, so that the pH decreases strongly from $\mathbf{c}^l$ to $\mathbf{c}^r$. Figure 9 shows the analytical and the numerical solutions for a case with the fundamental structure

$$\mathbf{c}^l \xrightarrow{\mathcal{S}_1} \mathbf{c}^m \xrightarrow{\mathcal{SR}_2} \mathbf{c}^r, \tag{5.5}$$

where $c_s^r = 0$. The numerical solution, which includes a diffusive flux, shows an additional wave at the leading edge of $\mathcal{SR}_2$ at $\eta = 1$. Previous simulations of dispersion-induced waves have used a different geochemical model, but Figure 9 shows that this phenomenon also occurs in this formulation. A detailed discussion of this dispersion-induced phenomenon, however, is beyond the scope of this work, which is focused on the hyperbolic structure.

6. Conclusions. In this paper, a theory for the solution of the Riemann problem for a one-dimensional, quasi-linear, 2×2 system of conservation laws describing reactive transport in a permeable medium with pH-dependent adsorption is developed. The conservation equation for protons contains a term accounting for the dissociation of water which introduces additional nonlinearity in the accumulation term. The system is strictly hyperbolic and nongenuinely nonlinear, because the pH-dependent adsorption isotherms are not convex functions. This leads to nine fundamental

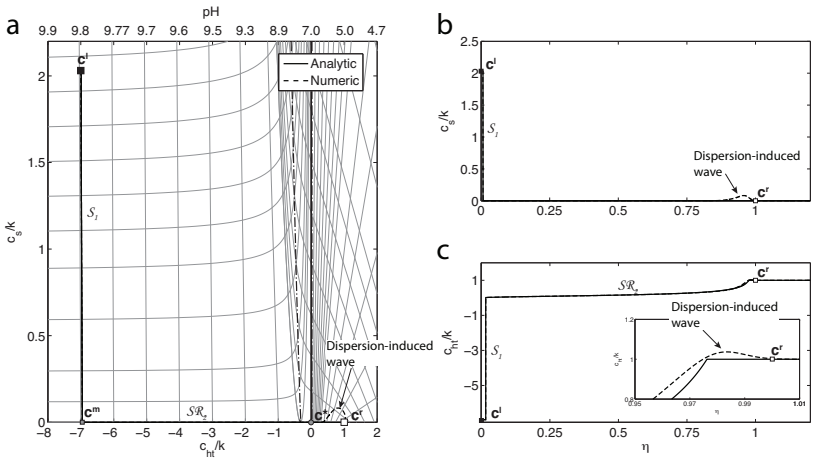

FIG. 9. *Nonclassical reactive transport behavior under the condition of* $c_s^r = 0$ *and for* $k_h = 10^{8.73}$, $k_s = 10^{4.47}$ *as in* [27].

solution structures, which are a concatenation of elementary and composed waves. Reactive transport with pH-dependent adsorption can, therefore, develop more complex reaction fronts than competitive adsorption of solutes with negligible complexation reactions. When both left and right states are at low pH (less than 7), however, the abundance of protons reduces the influence of the dissociation of water and the isotherms reduce to convex two-component Langmuir isotherms considered in chromatography. The classic solutions of chromatography are, therefore, a subset of the solutions discussed here. Numerical simulations show excellent agreement with the analytic solutions in the hyperbolic limit, but in certain cases the interaction of hydrodynamic dispersion and pH-dependent adsorption can lead to an additional wave traveling without retardation, as previously reported.

Appendix A. Total proton concentration. In an aqueous system, the three chemical species H_2O, H^+, and OH^- are linearly dependent and only two can be chosen as a basis to span the compositional space. In aqueous chemistry [24], H_2O and H^+ are usually chosen as basis and $OH^- = H_2O$ - H^+. Under the assumption of local chemical equilibrium, only the conservation equations for the basis species have to be considered. In addition, the concentration of water is assumed to be constant because the aqueous solution is assumed to be dilute, so that only the conservation equation for protons is required,

$$\frac{\partial}{\partial t}\left(c_{ht} + z_h\right) + \frac{\partial c_{ht}}{\partial x} = 0, \tag{A.1}$$

where z_h is the adsorbed proton concentration derived in Appendix B and the total concentration of the H^+ basis species in the aqueous phase is given by

$$c_{ht} = c_{H^+} - c_{OH^-}, \tag{A.2}$$

where the minus sign arises because the OH^- species is generated by subtracting the H^+ basis species from the H_2O basis species.

Appendix B. Geochemical model. We considered an aqueous system containing protons (H^+) and a general solute (S^{n+}) of positive charge, which can be adsorbed onto a reactive surface as

$$X^{-1/2} + H^+ \longleftrightarrow XH^{+1/2}, \tag{B.1}$$

$$X^{-1/2} + S^{n+} \longleftrightarrow XS^{n-1/2}, \tag{B.2}$$

where $X^{-1/2}$ corresponds to a reactive surface site [14]. Neglecting the electrostatic term of the effective equilibrium constant that accounts for the development of the surface charge upon adsorption, the effective equilibrium constants equal the intrinsic equilibrium constants (kg mol^{-1})

$$k_h = \frac{\{XH^{+1/2}\}}{c_h X^{-1/2}} = 10^8, \tag{B.3}$$

$$k_s = \frac{\{XS^{n-1/2}\}}{c_s\{X^{-1/2}\}} = 10^5, \tag{B.4}$$

where c_i corresponds to the concentrations of the subscripted species (mol kg^{-1}) and the equilibrium constants resemble those appropriate for the adsorption of strontium on iron oxide at 25°C in [34]. The surface site balance is given by

$$z_t = \{X^{-1/2}\} + \{XH^{+1/2}\} + \{XS^{n-1/2}\}, \tag{B.5}$$

where z_t is the total concentration of the reactive surface sites (mol kg^{-1}).

Combining (B.3), (B.4), and (B.5), the adsorbed concentration (mol kg^{-1}) of protons, z_h, and of the solute, z_s, on the reactive surface are

$$z_h = \frac{z_t k_h c_h}{1 + k_h c_h + k_s c_s}, \tag{B.6}$$

$$z_s = \frac{z_t k_s c_s}{1 + k_h c_h + k_s c_s}. \tag{B.7}$$

These functions resemble the two-component Langmuir isotherm employed in previous chromatographic studies [29, 26, 7, 33, 8, 2, 3, 23]. In pH-dependent sorption the isotherms have to be expressed in terms of the total concentration of protons in the fluid, c_{ht}, introduced in Appendix A, instead of the proton concentration, c_h.

Combining (A.2) with the law of mass action for the dissociation of water

$$H_2O \longleftrightarrow OH^- + H^+, \quad k_w = c_{oh}\, c_h = 10^{-14}, \tag{B.8}$$

we derive the expression

$$c_h = \frac{1}{2}\left(c_{ht} + \sqrt{c_{ht}^2 + 4k_w}\right), \tag{B.9}$$

which can be substituted into (B.6) and (B.7), to obtain the pH-dependent adsorption isotherms

$$z_h = \frac{\phi z_t k_h \frac{1}{2}\left(c_{ht} + \sqrt{c_{ht}^2 + 4k_w}\right)}{1 + k_h \frac{1}{2}\left(c_{ht} + \sqrt{c_{ht}^2 + 4k_w}\right) + k_s c_s}, \tag{B.10}$$

$$z_s = \frac{\phi z_t k_s c_s}{1 + k_h \frac{1}{2}\left(c_{ht} + \sqrt{c_{ht}^2 + 4k_w}\right) + k_s c_s}. \tag{B.11}$$

REFERENCES

[1] F. Ancona and A. Marson, *A note on the Riemann problem for general n×n conservation laws*, J. Math. Anal. Appl., 260 (2001), pp. 279–293.

[2] C. Appelo, J. Hendriks, and M. Vanveldhuizen, *Flushing factors and a sharp front solution for solute transport with multicomponent ion-exchange*, J. Hydrol., 146 (1993), pp. 89–113.

[3] C. Appelo, *Multicomponent ion exchange and chromatography in natural systems*, Reviews in Mineralogy, 34 (1996), pp. 193–227.

[4] T. Barkve, *The Riemann problem for nonstrictly hyperbolic system modeling nonisothermal, two-phase flow in a porous medium*, SIAM J. Appl. Math., 49 (1989), pp. 784–798.

[5] S. L. Bryant, C. Dawson, and C. van Duijn, *Dispersion-induced chromatographic waves*, Ind. Eng. Chem. Res., 39 (2000), pp. 2682–2691.

[6] B. J. Cantwell, *Introduction to Symmetry Analysis*, Cambridge University Press, Cambridge, UK, 2002.

[7] R. Charbeneau, *Groundwater contaminant transport with adsorption and ion-exchange chemistry—method of characteristics for the case without dispersion*, Water Resour. Res., 17 (1981), pp. 705–713.

[8] R. Charbeneau, *Multicomponent exchange and subsurface solute transport—characteristics, coherence, and the Riemann problem*, Water Resour. Res., 24 (1988), pp. 57–64.

[9] A. H. Falls and W. M.Schulte, *Features of three-component, three-phase displacement in porous media*, SPE Reserv. Eng., 7 (1992), pp. 426–432.

[10] E. Glueckauf, *Theory of chromatography; chromatograms of a single solute*, J. Chem. Soc., (1947), pp. 1302–1308.

[11] E. Glueckauf, *Theory of chromatography:* VII. *The general theory of two solutes following non-linear isotherms*, Discuss. of Faraday Soc., 7 (1949), pp. 12–25.

[12] J. Gruber, *Waves in a two-component system: The oxide surface as a variable charge adsorbent*, Ind. Eng. Chem. Res., 34 (1995), pp. 2769–2781.

[13] F. Helfferich and G. Klein, *Multicomponent Chromatography*, Marcel Dekker, New York, 1970.

[14] T. Hiemstra, J. Dewit, and W. Vanriemsdijk, *Multisite proton adsorption modeling at the solid-solution interface of (hydr)oxides—a new approach.* II. *Application to various important (hydr)oxides*, J. Colloid Interf. Sci., 133 (1989), pp. 105–117.

[15] E. Isaacson, D. Marchesin, B. Plohr, and J. B. Temple, *Multiphase flow models with singular Riemann problems*, Mat. Apl. Comput., 11 (1992), pp. 147–166.

[16] R. Juanes and T. Patzek, *Analytical solution to the Riemann problem of three-phase flow in porous media*, Transp. Porous Media, 55 (2004), pp. 47–70.

[17] R. Juanes and M. J. Blunt, *Analytical solutions to multiphase first-contact miscible models with viscous fingering*, Transp. Porous Media, 64 (2004), pp. 339–373.

[18] L. Lake, S. L. Bryant, and A. Araque-Martinez, *Geochemistry and Fluid Flow*, Elsevier, Amsterdam, The Netherlands, 2002.

[19] P. Lax, *Hyperbolic systems of conservation laws*, II., Comm. Pure Appl. Math., 10 (1957), pp. 537–566.

[20] R. J. LeVeque, *Numerical Methods for Conservation Laws*, 2nd ed., Birkhäuser, Berlin, 2008.

[21] T. Liu, *The Riemann problem for general* 2×2 *conservation laws*, Trans. Amer. Math. Soc., 199 (1974), pp. 89–112.

[22] P. C. Lichtner, *Continuum formulation of multicomponent-multiphase reactive transport*, Reviews in Mineralogy, 34 (1996), pp. 1–81.

[23] M. Mazzotti, *Local equilibrium theory for the binary chromatography of species subject to a generalized Langmuir isotherm*, Ind. Eng. Chem. Res., 45 (2006), pp. 5332–5350.

[24] F. M. M. Morel and J. G. Hering, *Principles and Applications of Aquatic Chemistry*, John Wiley and Sons, New York, 1993.

[25] F. J. Orr, *Theory of Gas Injection Processes*, Tie-Line Publications, Holte, Denmark, 2007.

[26] G. Pope, L. Lake, and F. Helfferich, *Cation-exchange in chemical flooding. Part* 1. *Basic theory without dispersion*, Soc. Petrol. Eng. J., 18 (1978), pp. 418–434.

[27] V. Prigiobbe, M. A. Hesse, and S. L. Bryant, *Anomalous reactive transport in the framework of the theory of chromatography*, Transp. Porous Med., 93 (2012), pp. 127–145.

[28] V. Prigiobbe, M. A. Hesse, and S. L. Bryant, *Fast strontium transport induced by hydrodynamic dispersion and pH-dependent sorption*, Geophys. Res. Lett., 39 (2012), L18401.

[29] H. K. Rhee, A. Aris, and N. Amudson, *First-Order Partial Differential Equations, Vol.* II, *Theory and Application of Hyperbolic Systems of Quasilinear Equations*, Prentice-Hall, Englewood Cliffs, NJ, 1989.

[30] B. Temple, *Systems of conservation laws with coinciding shock and rarefaction curves*, Contemp. Math., 17 (1983), pp. 143–151.

[31] L. Toran, S. L. Bryant, J. Saunders, and M. Wheeler, *A two-tiered approach to reactive transport: Application to Sr mobility under variable pH*, Ground Water, 36 (1998), pp. 404–408.

[32] D. Tandeur and G. Klein, *Multicomponent ion exchange in fixed beds*, Eng. Chem. Fund., 6 (1967), pp. 351–361.

[33] A. Valocchi, R. Street, and P. Roberts, *Transport of ion-exchanging solutes in groundwater—chromatographic theory and field simulation*, Water Resour. Res., 17 (1981), pp. 1517–1527.

[34] W. van Beinum, A. Hofmann, J. Meeussen, and R. Kretzschmar, *Sorption kinetics of strontium in porous hydrous ferric oxide aggregates* I. *The Donnan diffusion model*, J. Colloid Interf. Sci., 283 (2005), pp. 18–28.